A High-Granularity Timing Detector for the ATLAS Phase-II upgrade

M.P. Casado[a], on behalf of the ATLAS HGTD Group[b]

[a]*Departament de Física, Universitat Autònoma de Barcelona, Institut de Física d'Altes Energies and Barcelona Institute of Science and Technology, Spain.*

Abstract

The increase of the particle flux at the HL-LHC with instantaneous luminosities up to L = 7.5×10^{34} cm^{-2} s^{-1} will have a severe impact on the ATLAS detector reconstruction and trigger performance. The end-cap and forward region where the liquid Argon calorimeter has coarser granularity and the inner tracker has poorer momentum resolution will be particularly affected. A High Granularity Timing Detector will be installed in front of the LAr end-cap calorimeters to help in charged-particle reconstruction and luminosity measurement. This low angle detector is introduced to augment the new all-silicon Inner Tracker in the pseudo-rapidity range from 2.4 to 4.0. Two silicon-sensor double-sided layers per side will provide precision timing information for minimum-ionising particles with a resolution as good as 30 ps per track in order to assign each particle to the correct vertex. Readout cells have a size of 1.3 mm × 1.3 mm, leading to a highly granular detector with 3.7 million channels. The Low Gain Avalanche Detectors technology has been chosen as sesor chip as it provides excellent timing performance. The requirements and overall specifications of the High Granularity Timing Detector will be presented as well as the technical design and the project status. The on-going R&D effort carried out to study the sensors, the readout ASIC, and the other components, supported by laboratory and test beam results, will also be presented.

Keywords: HL-LHC, ATLAS, HGTD, pp collisions

1. Introduction

The High-Luminosity LHC (HL-LHC) [1] is expected to start operation in 2027. It will achieve an instantaneous luminosity of 7.5×10^{34} cm^{-2}s^{-1} and will collect an integrated luminosity of 4 000 fb^{-1}. With such beam conditions the average number of interactions per collision will be typically 200, about one order of magnitude larger than during Run 2.
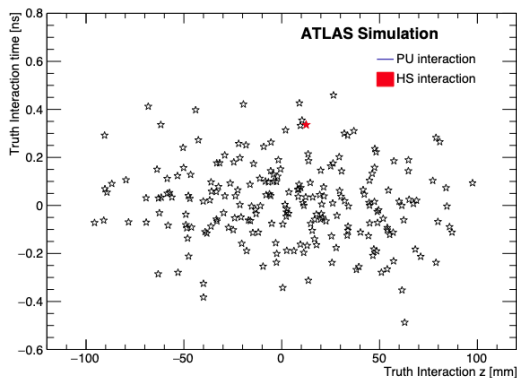

Figure 1: Visualisation of the truth interactions in a single bunch crossing in the z-t plane, showing the simulated Hard Scatter (HS) $t\bar{t}$ event interaction (red) with pile-up interactions superimposed (black) for < μ >= 200, from Ref. [3].

The ATLAS detector [2] will undergo a number of upgrades to cope with the HL-LHC running environment. The Data Acquision (DAQ) and Trigger systems will improve their granularity and will have faster electronics achieving an output rate of 10 kHz. The current inner tracker will be replaced by a fully silicon based detector (ITk), and its acceptance will be extended up to pseudo-rapidity equal to 4. The calorimeters will be partially upgraded with more granular and faster electronics. In the end-cap region the electronics of the muon chambers will also be replaced to cope with the new conditions. Finally, a High Granularity Timing Detector (HGTD) [3] is planned for the forward region of the ATLAS detector where the performance of the calorimeters and ITk is particularly degraded. HGTD will perform timing measurements of charged tracks and help in the suppression of pile-up.

The High Granularity Detector will provide a time resolution of 30 ps for tracks in the forward region and will be able to reject pile-up from $|\eta| = 2.4$ to $|\eta| = 4$ by exploiting the track timing information (see Figure 1) . More generally, this detector will improve the performance of the ATLAS detector in the forward region to a level comparable to that for $|\eta| < 2.4$ and provide a powerful tool for luminosity measurement.

These proceedings will briefly describe the HGTD geometry and running conditions in section 2, discuss the Low Gain Avalanche Detectors (LGAD) sensors and the detector layout in section 3, ASICs in section 4, performance and a few physics cases in section 5, and conclude in section 6.
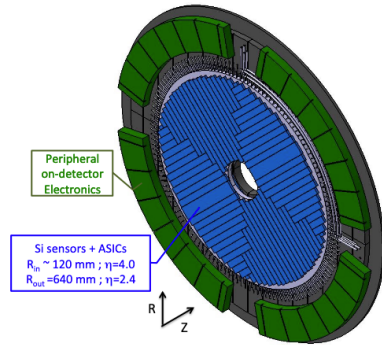
Figure 2: Illustration of the HGTD. The blue (green) region represents the active (off detector electronics) part of the detector, from Ref. [4].

2. Detector

The HGTD will be built in front of the end-cap calorimeters cryostats of ATLAS, at a distance of ±3.5 m of the interaction point and will cover the pseudo-rapidity region from 2.4 to 4 as shown in Figure 2. The space to build this detector is quite limited, its active radius goes from 120 mm to 640 mm and its thickness should not exceed 125 mm including 50 mm of moderator to protect the ITk and the HGTD from back-scattered neutrons. In order to ensure a timing resolution of 30 ps per track over all the HL-LHC (which might be degraded to 50 ps at the end of HL-LHC), two layers of active sensors will be built with an additional effective layer at low radius. This additional effective layer will provide 2.6 (2.0) hits per track at small (large) radii. This increase in the number of hits will be achieved by increasing the overlap of the modules for R < 230 mm from 20% to 70%.

Due to the high particle rate in the HGTD region it is crucial for the detector to be radiation hard. At the end of the HL-LHC the maximum neutron-equivalent fluence at a radius of 120 mm will reach 9×10^{15} n_{eq}/cm^2 (see Figure 3) including a safety factor of 1.5. That fluence decreases exponentially as function of the radius. The radiation dose (see Figure 4) will damage the electronics and the sensors, leading to a decrease of the timing resolution as a function of integrated luminosity. To maintain a sufficiently precise timing resolution the sensors and the ASICs will be replaced every 1 000/fb for the inner ring (120 mm < R < 230 mm), every 2 000/fb for the middle ring (230 mm < R < 470 mm), while the outer ring will not need to be replaced. In this scenario, the maximum fluence that the sensors have to sustain is 2.5×10^{15} n_{eq}/cm^2 (including a safe factor of 1.5).

3. Sensors

The HGTD sensors will be made of Low Gain Avalanche Detectors (LGAD) [5]. LGADs are n-on-p silicon detectors containing an extra highly-doped p-layer below the n-p junction to create a high field which causes internal amplification as displayed in Figure 5(a). When a charged particle crosses the
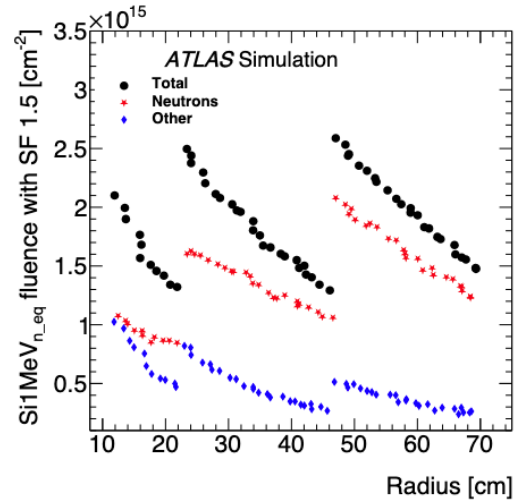

Figure 3: Si1MeV$_{neq}$ fluence for HL-LHC with scale factor applied and considering replacements, from Ref. [3].
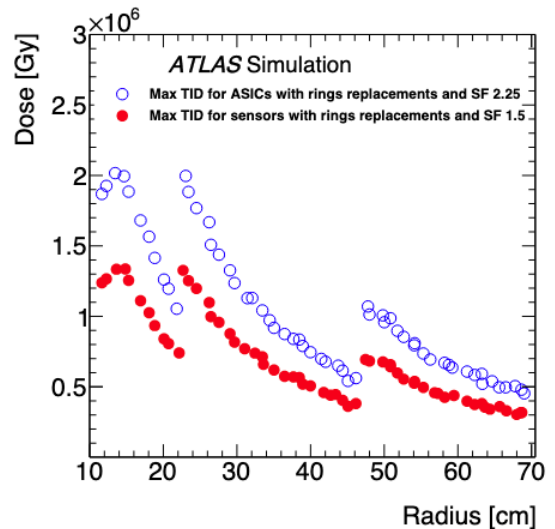

Figure 4: Ionising dose for HL-LHC with scale factor applied and considering replacements, from Ref. [3].
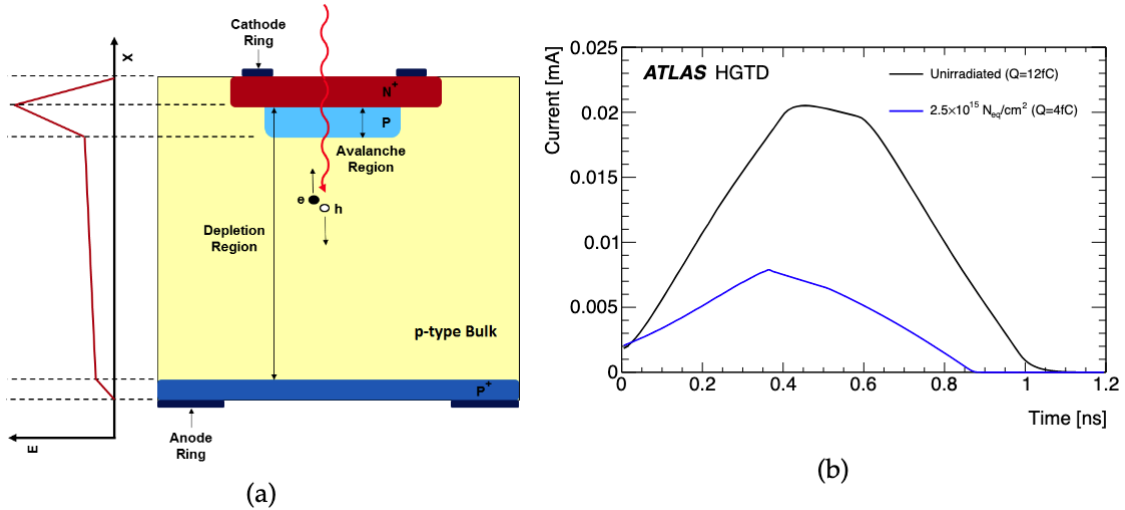
Figure 5: Cross section of an LGAD (a) and simulated signal current in LGADs at start and after full integrated neutron fluence (b), from Ref. [3].

detector, an initial current is created by the drift of the electrons and holes in the silicon. When the electrons reach the amplification region, new electron/hole pairs are created and the holes drift towards the p+ region and generate a large current. This charge amplification is referred to as the gain of the LGAD. This current, larger than in a standard diode, is the key ingredient to get an excellent time resolution for energy deposited by Minimum Ionizing Particles (MIP). The expected currents for different irradiation levels (therefore different gains) are presented in Figure 5 (b). For large gain, the rise time is about 500 ps and the signal duration is approximately 1 ns. When the irradiation neutron fluence increases, the charge is smaller and the rise time and the signal duration are shorter.

After amplification in the gain layer, the height of the LGAD signal is proportional to the gain. On the other hand, the slope dV/dt depends on the thickness of the sensor, favouring thin sensors since the electronics jitter scales as the inverse of the slope [3]. However, the jitter also depends linearly on the detector pad capacitance, therefore limiting the potential use of very thin sensors. Consequently, the optimal thickness relies strongly on the performance of the read-out ASIC. The baseline active thickness has been chosen to be 50 μm, the total thickness is 300 μm and the pad size 1.3×1.3 mm^2.

Over the last five years LGAD sensors have been produced by CNM/Spain, HPK/Japan, FBK/Italy and recently NDL and IME/China, with different doping levels, active thicknesses, pad sizes, and inter-pad gaps. These detectors have been exposed to protons, neutrons and X-rays up to the expected maximum radiation levels (including the safety factors) and intensively characterized in the laboratory (with probe stations, β sources and lasers) and in beam tests (at CERN, DESY, Fermilab).

Figure 6 summarizes the time resolution obtained in the laboratory measurements, with dedicated electronics, for sensors from different producers exposed to a neutron fluence up to 2.5 $\times 10^{15}$ n$_{eq}$ cm^{-2}. A charge of 4 fC can be reached up to a fluence of 3×10^{15} n$_{eq}$ cm^{-2}, providing a time resolution smaller than
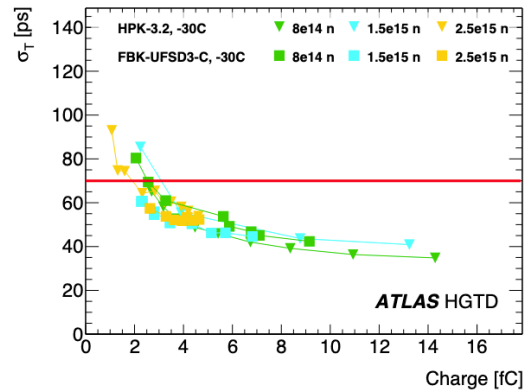

Figure 6: Time resolution as a function of the collected charge for neutron irradiated LGADs from different producers (HPK, FBK) with a 50 μm active thickness. These measurements have been made at -30°C, in the laboratory with a β source using a custom electronics read-out board (not the ALTIROC therefore optimistic with respect to the expected electronics jitter contribution). The typical error bar is about 3 ps. The red line shows that in these conditions better than 70 ps time resolution is obtained at 4 fC. Figure taken from Ref. [3].
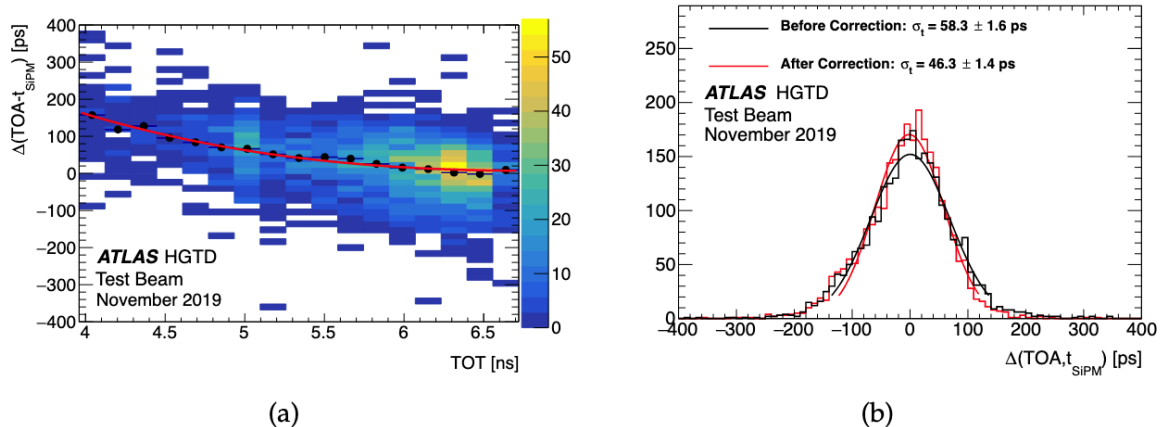
3

(a)

(b)

Figure 7: (a): Distribution of the time-of-arrival (TOA) as a function of the time-over-threshold (TOT). The dots correspond to the mean value of the TOA distribution for a given TOT bin extracted from a Gaussian fit. The red line is a fit of the average TOA as a function of the TOT. (b): Distributions of the time difference between LGAD+ALTIROC and the Quartz+SiPM system before (red) and after (black) time walk correction together with Gaussian fits. The numbers are the fitted Gaussian widths where the time resolution of the Quartz+SiPM system has been subtracted quadratically. Figures taken from Ref. [3].

70 ps per hit. The performance of sensors from all manufacturers is similar, even if before irradiation the optimal operating bias voltage might be different because the doping profile is different. With a minimal charge of about 4 fC and a discriminator threshold of about 2 fC, a hit efficiency of at least 95% is expected.

4. ASICs

The front-end electronics is constituted by ATLAS TIming ReadOut Chip (ALTIROC), an ASIC chip bump bonded to the LGAD sensor. It will have 225 readout channels, thus two ASICs will read out each LGAD. The main challenge in the design of this ASIC is the fact that it needs to have a small contribution to the timing resolution, in order to match the excellent performance of the LGAD.

A version of ALTIROC, the ALTIROC1v2 ASIC, bump bonded to a LGAD sensor array (HPK 3.1) was exposed to electron beam tests at DESY in fall of 2019. The LGADs were operated with a bias voltage of 230 V, resulting in a MIP charge deposit of about 20 fC.

Figure 7 (a) shows the time-of-arrival (TOA) variation as a function of the time-over-threshold (TOT). The range of the TOT is truncated since it was not possible to measure large values of TOT because of a coupling between the busy signal of the TOA TDC and the falling edge of the preamplifier output. This coupling only occurs when this signal is output on the PCB. This TOA busy signal must be output during test beam in order to synchronize the data from ALTIROC and the oscilloscope used to record the Quartz+SiPM system waveforms. This signal won't be needed for the HGTD and is not used for test bench measurements (it is only used for debug purposes). In the next iteration, ALTIROC1v3, the busy signal will be output as a differential signal to solve this problem. Therefore, with ALTIROC1v2, only a range of the TOT can be used in test beam

and Figure 7 (a) also displays a fit in this restricted range used for the time walk correction.

Figure 7 (b) shows the time difference between LGAD+ALTIROC hybrid and the reference time from the Quartz+SiPM system before and after the time walk correction extracted from the fit in Figure 7 (a). The distributions are Gaussian without any tails. The measured time resolution decreases from 58.3±1.6 ps to 46.3±1.4 ps after time walk correction. Subtracting the Landau contribution (about 25 ps), the remaining time resolution is about 39 ps containing contributions from the electronics jitter, TDC and clocks. These are encouraging results, but it is important to measure the performance of full sized devices (15x15 pads) before and after irradiation. The first full size ASIC prototype (ALTIROC2) has been fabricated and is already being tested by the HGTD Group.

5. Performance

The precise timing measurement of the HGTD can be used to greatly improve the reconstruction of different physics objects. This can be achieved by rejecting out of time pile-up that could contaminate objects thus reducing their reconstruction efficiency. In order to study the performance of the HGTD and optimize the detector layout, fully simulated events [6] of single muons, single electrons, single pions, jets, inelastic p-p interactions and several other physics processes have been produced.

The pile-up rejection has been evaluated in different jet p_T regimes and pseudorapidty intervals. It has been shown that HGTD can introduce an improvement of up to a factor 4 if a timing resolution per track of 30 ps is assumed [3].

Heavy-flavour tagging is another area which is critical in HL-LHC era. The b-tagging algorithms are particularly sensitive to pile-up contamination. The b-jets are associated with a displaced vertex so the algorithms accept tracks with a very large impact parameter (z_0) window and thus increase the likeliness

of using pile-up tracks. Using the HGTD timing information a fraction of the pile-up tracks in this z_0 window is rejected and the identification of b-jets in the forward region is improved by a factor 1.4 to 1.8 [3].

The HGTD can be used to improve the identification of the leptons in the forward region. When working with leptons it is important to know if they originate from the hard scatter event or if they are the result of a decay, a conversion or a fake. In Ref [3] it is show how HGTD can improve the selection efficiency for electron isolation criteria by about 10%.

HGTD can also help in physics analyses that can benefit from improved jet and lepton reconstruction, as for example Standard Model measurements of a VBS process and the weak mixing angle $\sin^2 \theta_{\text{eff}}$, and a search for VBF-produced Higgs bosons decaying invisibly. In the measurement of $\sin^2 \theta_{\text{eff}}$, HGTD reduces the total experimental uncertainty by 11% [3].

In the search for VBF-produced Higgs bosons decaying invisibly HGTD can improve the S/B ratio, as shown in Figure 8. This figure is normalized to ITk-only performance. For a particular pile-up jet efficiency gain from the application of HGTD relative to ITk, the dotted blue line shows the corresponding gain in S/B. For example, a 20% increase in forward pile-up rejection for jets above 50 GeV (without any loss in hard-scatter efficiency), would correspond to a S/B gain of approximately 15% (corresponding to the y-axis when the horizontal value is 0.80).
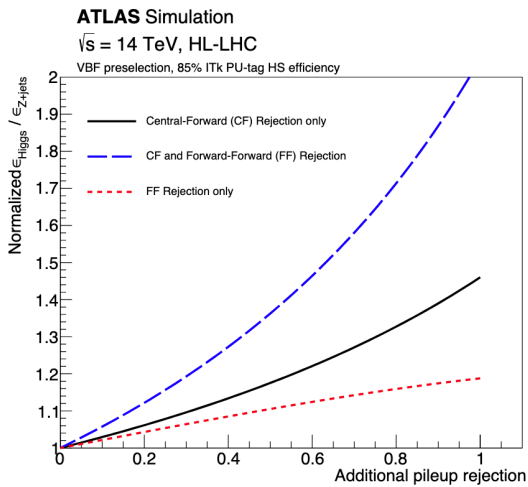

Figure 8: Normalized signal over background gain relative to ITk-only pile-up jet suppression performance, as a function of the additional pile-up jet rejection from HGTD. The solid black (dotted red) line represents the HGTD improvement from the Central-Forward (Forward-Forward) event topologies separately. The dotted blue line shows the total improvement when the combined HGTD+ITk pile-up suppression algorithm is applied to all jets in the event. Figure taken from Ref. [3].

In addition to improving the reconstruction of physics objects, the HGTD can also be used as a luminosity measurement device. Since this detector is highly granular and has a low occupancy a good linearity between the number of hits in the detector and the number of interactions per bunch crossing is expected.

With the HGTD a precise measurement of luminosity is possible by integrating all the hits in a period of 1s. A statistical precision of 0.14% for a run with an average number of simultaneous pp interactions, $< \mu >= 1$ and down to 0.01% for a run with $< \mu > = 200$ is possible. Better precision could also be achieved through a longer averaging time.

6. Conclusion

The HGTD will cover the forward region of the ATLAS detector in $|\eta|$ between 2.4 and 4.0, providing a timing resolution of 30 ps per minimum-ionizing particle. This detector is proposed to be built using LGAD sensors with a pixel size of 1.3×1.3 mm^2. The timing information provided by this detector will be used to mitigate the effects of the pile-up in the forward region, improving the reconstruction of physics objects to a level similar to the one obtained in the central region. The HGTD will also provide luminosity measurements online and offline.

References

[1] G. Apollinari, I. Béjar Alonso, O. Brüning, M. Lamont, L. Rossi (Eds.), *High-Luminosity Large Hadron Collider (HL-LHC): Preliminary Design Report*, CERN-2015-005, https://cds.cern.ch/record/2116337/files/CERN-2015-005.pdf.

[2] ATLAS Collaboration, *The ATLAS Experiment at the CERN Large Hadron Collider*, JINST **3** S08003 (2008), https://iopscience.iop.org/article/10.1088/1748-0221/3/08/S08003/pdf.

[3] ATLAS Collaboration, *Technical Design Report: A High-Granularity Timing Detector for the ATLAS Phase-II Upgrade*, CERN-LHCC-2020-007 ; ATLAS-TDR-031, Geneva, Feb, 2021, https://cds.cern.ch/record/2719855/files/ATLAS-TDR-031.pdf.

[4] C. Allaire, *A High-Granularity Timing Detector (HGTD) in ATLAS: Performance at the HL-LHC*, ATL-LARG-PROC-2018-003, CERN, Geneva, Feb, 2018, https://cds.cern.ch/record/2302827/files/ATL-LARG-PROC-2018-003.pdf.

[5] H. F. W. Sadrozinski, A. Seiden, N. Cartiglia, *4D tracking with ultra-fast silicon detectors*, Rept. Prog. Phys. 81 (2) (2018) 026101. arXiv:1704.08666, doi 10.1088/1361-6633/aa94d3.

[6] ATLAS Collaboration, *The ATLAS Simulation Infrastructure*, Eur. Phys. J. C 70 (2010) 823. arXiv:1005.4568, doi:10.1140/epjc/s10052-010-1429-9.